

Renewable Hydrochar Adsorbent for Applications in Lead Removal

A Major Qualifying Project Report

Submitted to the faculty of

WORCESTER POLYTECHNIC INSTITUTE

In partial fulfillment of the requirements for the degree of

Bachelor of Science

By

Lili Hellerman

Andrew Troup

Report submitted to

Professor Michael Timko

Date:

April 25, 2024



WPI



SOMAX

This report represents the work of WPI undergraduate students submitted to the faculty as evidence of completion of a degree requirement. WPI routinely publishes these reports on its website without editorial or peer review. For more information about the projects program at WPI, please see <http://www.wpi.edu/academics/ugradstudies/project-learning.html>

Abstract

This report examines the adsorption capacity of sewage sludge based hydrochar for lead. A sewage sludge-based adsorbent for lead removal targets two major environmental issues, organic waste disposal and lead pollution. The methods for the experiments outlined in this report were based on previous work completed by Hunter Wieckowski on the adsorption capacity of sewage sludge based Hydrochar for copper. The adsorption data for lead was fit to two major adsorption models: Langmuir and Freundlich. Both empirical models had similar goodness of fits, with the Freundlich model fitting the data slightly better than the Langmuir model. Comparing the adsorption data for lead and copper showed that the adsorption of lead was higher than copper at equilibrium concentrations less than 0.2 mg/g and less than copper at equilibrium concentrations greater than 0.2 mg/g. The max adsorption capacity of sewage sludge hydrochar for lead was found to be 9.19 mg/g and was compared to the max adsorption capacity for other hydrochar materials.

Acknowledgements

We would like to thank Worcester Polytechnic Institute for sponsoring this project and SoMax Circular solutions for providing us with all the hydrochar needed to perform the experiments. We would also like to thank our principal investigator Professor Michael Timko and our graduate student advisor, Karen Argo for their continued support throughout its completion. In addition, we would like to thank Professor Geoffrey Tompsett and Don Pellegrino for supporting us in the lab.

Table of Contents

Abstract	I
Acknowledgements	II
Table of Contents	III
Table of Figures.....	IV
1. Background	1
1.1 Heavy Metal Contamination.....	1
1.1.1 Lead Pollution.....	2
1.2 Adsorption.....	3
1.2.1 Adsorption Mechanism.....	4
1.2.2 Adsorbent Materials	5
1.3 Hydrochar	6
1.3.1 Carbon Precursors	7
1.3.1 Hydrothermal Carbonization.....	9
1.4 Previous work	10
2. Methods.....	11
2.1 Sample Adsorption.....	11
2.2 Sample Filtration and Dilution	12
2.3 Measurement and Data Analysis.....	15
3. Results and Discussion	17
3.1 Lead Isotherm	18
3.2 Langmuir Adsorption.....	19
3.3 Freundlich Adsorption	21
3.4 Comparisons to Additional Hydrochar	23
4. Conclusion.....	25
5. Recommendations.....	26
References	28

Table of Figures

Table 1.1: Maximum Contaminant Level (MCL) and Health effects of Heavy Metal contaminants in drinking water [21]	2
Figure 1.2. Biosolids Use & Disposal from 2022 Biosolids Annual Reports [11].....	8
Table 1.2: Thermochemical process characteristics (a: [27] , b: [28], c: [30]).....	9
Figure 2.1. (a) samples with hydrochar before shaking and (b) samples with hydrochar after shaking	12
Figure 2.2. Vacuum filtration apparatus.....	13
Figure 2.3. Syringe filtration of samples.	14
Figure 2.4. Diagram depicting the three serial dilutions performed for the experiments.	15
Figure 3.1 A graph of adsorption capacity, Q_e , as a function of the equilibrium concentration, C_e . The data for both copper and lead are displayed with the calculated Langmuir and Freundlich adsorption models.	17
Figure 3.3 A graph of the Adsorption capacity SoMax sewage sludge hydrochar, Q_e , as a function of the equilibrium concentration, C_e	18
Figure 3.4. A graph of the Adsorption capacity SoMax sewage sludge hydrochar, Q_e , as a function of the equilibrium concentration, C_e . The graph only contains significant data.....	19
Figure 3.6. The linearization of the lead adsorption data and line of best fit to find the Freundlich variables.	22
Figure 3.8 A graphical comparison of the Freundlich adsorption coefficient, K_F , of both lead and copper for the adsorption as modeled by the Freundlich isotherm.	23

1. Background

As the push for global sustainability changes grows, political leaders and scientists, now more than ever, hold the stability of the future world climate in their hands. Recently, scientists have begun to use new and innovative technology to address environmental issues. Heavy metals pose a significant threat to both human and environmental health [3]. Anthropogenic actions related to industrialization, agriculture, and urbanization are responsible for the increases in heavy metal pollution worldwide [20]. Carbon based adsorbent materials produced from thermochemical processes are widely used for heavy metal removal [7]. Furthermore, waste management poses a risk to ecosystems and humans with the increasing volume and complexity of wastes [9,10]. As a result of its high moisture content, sewage sludge is one of the more difficult types of waste to manage via conventional processes [16]. Hydrothermal carbonization (HTC) has emerged as an economically favorable and sustainable process for treating sewage sludge due to its favorability towards materials with high moisture content and lower operating costs [16]. Hydrochar is the solid product of HTC and has applications in many fields including wastewater treatment and heavy metal removal [16]

1.1 Heavy Metal Contamination

According to 163 credible reports published between 2016 and 2021, heavy metals occur most frequently in polluted sites among inorganic contaminants [8]. Heavy metals frequently reported in contaminated sites of concern are lead (Pb), cadmium (Cd), arsenic (As), mercury (Hg), chromium (Cr), copper (Cu), manganese (Mn), iron (Fe), silver (Ag), vanadium (V), and zinc (Zn) [8]. Due to their atomic structures, heavy metals are highly

reactive and have the tendency to form complexes with other molecules [21]. These chemical properties make heavy metals one of the most biologically dangerous and toxic contaminants [21]. As a result, heavy metals are strictly regulated by the Environmental Protection Agency (EPA) and other environmental agencies worldwide [21]. Table 1.1 outlines the EPA Maximum Contaminant Limits (MCL) and negative health effects of heavy metals commonly found in contaminated wastewater. This report focuses on lead and copper contamination of water.

Table 1.1: Maximum Contaminant Level (MCL) and Health effects of Heavy Metal contaminants in drinking water [21]

Heavy Metal	MCL (mg/L)	Negative Health Effects
Arsenic (As)	0.05	Skin and vascular diseases, visceral cancer
Cadmium (Cd)	0.01	Renal disorders and damage, carcinogenic
Chromium (Cr)	0.05	Headache, Diarrhea, Nausea, Carcinogenic
Copper (Cu)	0.25	Liver damage, Wilson’s disease, Insomnia
Mercury (Hg)	3.0×10^{-5}	Rheumatoid arthritis, circulatory & nervous disorders
Nickel, (Ni)	0.20	Dermatitis, Chronic Asthma, Carcinogenic
Lead (Pb)	6.0×10^{-3}	Cerebral disorders, Renal, Circulatory & Nervous System disorders
Zinc (Zn)	0.80	Depression, lethargy, neurological signs, increased thirst

The following sections discuss the impact of lead pollution and how heavy metal contaminants impact the disposal of sewage sludge.

1.1.1 Lead Pollution

According to the World Health Organization, lead exposure accounts for 21.7 million years lost to disability and death worldwide [1]. Lead is persistent and has a half-

life of 30 days in soft tissue and 10-20 years in bone [2]. Bioaccumulation of lead can even occur in the body from very small amounts of lead exposure a lifetime. Lead is second on the prioritized substance list by the agency for toxic substances and disease registry due to its toxic, mutagenic and carcinogenic potential [3]. The primary pathways for human lead exposure are through atmospheric dust, automobile exhaust, paint, and contaminated food and water [4]. Industrial sources of lead that contribute to soil and water contamination include electroplating and finishing, battery manufacturing and recycling, lead pipe manufacturing and recycling, and mining [5]. More than 20% of a person's lifetime lead exposure is from drinking water [6]. Lead exposure from drinking water is preventable with the implementation of heavy metal removal technology.

1.2 Adsorption

The methods of heavy metal removal can be formed into five categories: adsorption-, membrane-, chemical-, electric-, and photocatalytic- based treatments [7]. According to Naef A. A. Qasem et al., adsorption is the most promising method for removing heavy metal ions [7]. There are two types of adsorption: physical and chemical [21]. Physical adsorption occurs via weak Van Der Waals attraction forces with no chemical reaction taking place between adsorbent and adsorbate [21]. Chemical adsorption, or chemisorption, is caused by ionic and covalent chemical reactions between adsorbent and adsorbate [21]. Physical adsorption is less specific and highly reversible, whereas chemical adsorption is selective and generally irreversible [21]. The advantages of the adsorption removal method are simple operation, strong applicability, high removal rate, and the low cost of reusability [7]. The following sections discuss the mechanism for

heavy metal adsorption onto carbon-based adsorbents and how the process is impacted by adsorbent materials.

1.2.1 Adsorption Mechanism

Heavy metal adsorption onto a carbon adsorbent involves both chemical and physical adsorption [23]. Physical adsorption (physisorption) is the result of weak intermolecular forces (i.e. Van Der Waals) between the surface of the adsorbent and the heavy metal ion [22]. The physical adsorption is directly proportional to the surface area of the adsorbent material, which increases with porosity and surface area of the material [22]. The chemical adsorption of heavy metals occurs via electrostatic interaction, ion exchange (redox reactions), hydrogen bonding, acid-base interaction, and complexation with the adsorbent [23]. Chemical adsorption takes place between the adsorbate (heavy metal ions) and the functional groups on the surface of the adsorbent (carbon material) [22]. Most functional groups on carbon-based adsorbents are negatively charged and include hydroxyl, carboxyl, carbonyl, and amino groups [22]. Almost all heavy metals have a positive oxidation number and exist as a positively charged ion in solution [22]. The resulting electrostatic interactions between the negatively charged surface groups and positively charged metal ions contribute to the adsorption capacity of the material [22]. Figure 1.1 shows the various types of adsorptions between heavy metals and carbon adsorbents.

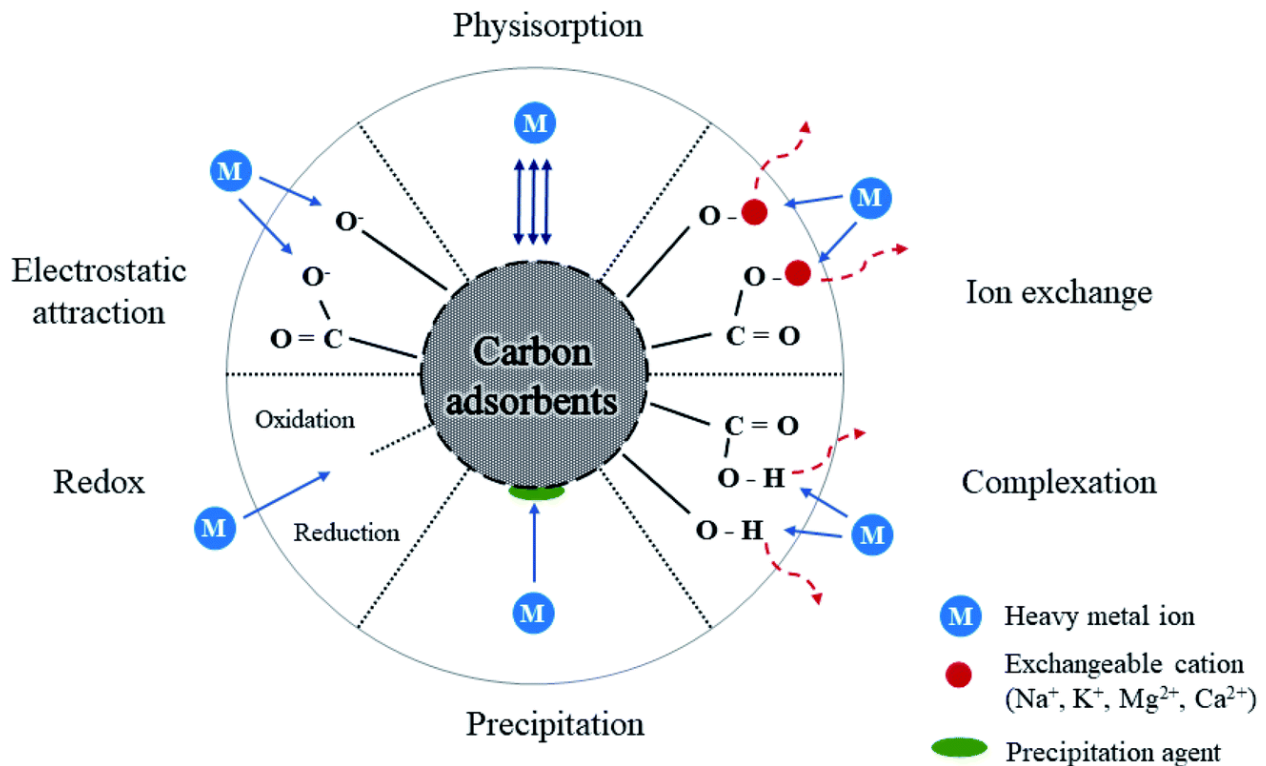


Figure 1.1. Diagram showing the different mechanisms of heavy metal adsorption from wastewater [24]

The mix of chemical and physical adsorption mechanisms means that both the morphological structure of the material and the presence and type of surface functional groups impact adsorption capacity [23]. The porosity and surface area and types of surface functional groups are impacted by different treatment methods but are primarily determined by the type of carbon adsorbent material used [23].

1.2.2 Adsorbent Materials

The efficiency and effectiveness of adsorption methods depends on the selection of low-cost and high performing adsorbent materials [7]. The high performance of adsorbent materials depends on the surface area, porosity, and surface functional groups [21]. High surface area and high porosity increase physisorption via the facilitation of contaminant diffusion onto the surface of the adsorbent [25]. The nature and number of

functional groups determines the surface chemistry, which is the primary factor affecting the chemical adsorption mechanisms [25]. Carbon-based adsorbents are extensively used in applications for heavy metal removal due to their high specific surface area, well-developed pore structure and presence of functional groups that are favorable for heavy metal adsorption [7][21]. Three of the widely used adsorbents are activated carbon, carbon nanotubes and graphene [7]. However, activated carbons are the most widely used carbon adsorbent due to favorable adsorption properties such as high specific surface area and presence of surface functional groups [21]. Activated carbon is formed from pyrolysis and the chemical activation of almost any carbon-rich material, providing opportunities for repurposing, and reducing waste [21]. Conventional carbon precursors include coal, wood, and a variety of agricultural wastes [22]. Carbon-based adsorbents differ depending on their production method. The drive towards a more sustainable future has led researchers to investigate alternatives for activated carbon in both production methods and materials.

1.3 Hydrochar

Hydrochar is a solid carbonaceous material produced from hydrothermal carbonization (HTC) and is a lower cost alternative to activated carbon [31]. Similar to activated carbons, hydrochar can be made from a variety of carbon-rich materials [17]. Hydrothermal carbonization is a thermochemical process upon which carbon material is heated to 180-200°C while submerged under water at saturated pressure [17]. Solid hydrochar is the primary product of hydrothermal carbonization but the process also produces a liquid product rich in nutrients and a gaseous product that is primarily CO₂

[30]. The potential advantages of recycling sewage sludge as a biosolid are outlined below.

1.3.1 Carbon Precursors

According to K. Fic et al., the most influential factors when producing hydrochar and other carbon-based adsorbents are the availability and cost of carbon precursors [12]. Hydrochar made from biosolids has promising applications in water treatment due to the increased functional groups from hydrolysis and recombination reactions of biomass monomers [26]. Biosolids are organic matter recycled from sewage sludge and contain 50-70% carbon and other organic materials with trace amounts of inorganic contaminants [11]. With the US alone managing 3.76 million dry metric tons of sewage sludge in 2022, biosolids are a widely available carbonaceous material and easily accessible for wastewater applications [11].

1.3.1.1 Sewage Sludge

With improvements in wastewater treatment technologies and increased effluent quality, the volume of sewage sludge produced each year has increased [9]. Communities around the world struggle with disposal of sewage sludge, especially as the availability of conventional disposal methods dwindle and costs increase [9]. Sewage sludge is composed of both organic materials and inorganic materials [10]. Sludge that has undergone both mechanical (dewatering) and chemical (stabilization and pathogen removal) treatment is then classified as biosolids [10]. The disposal methods of biosolids in the US are shown in figure 1.2.

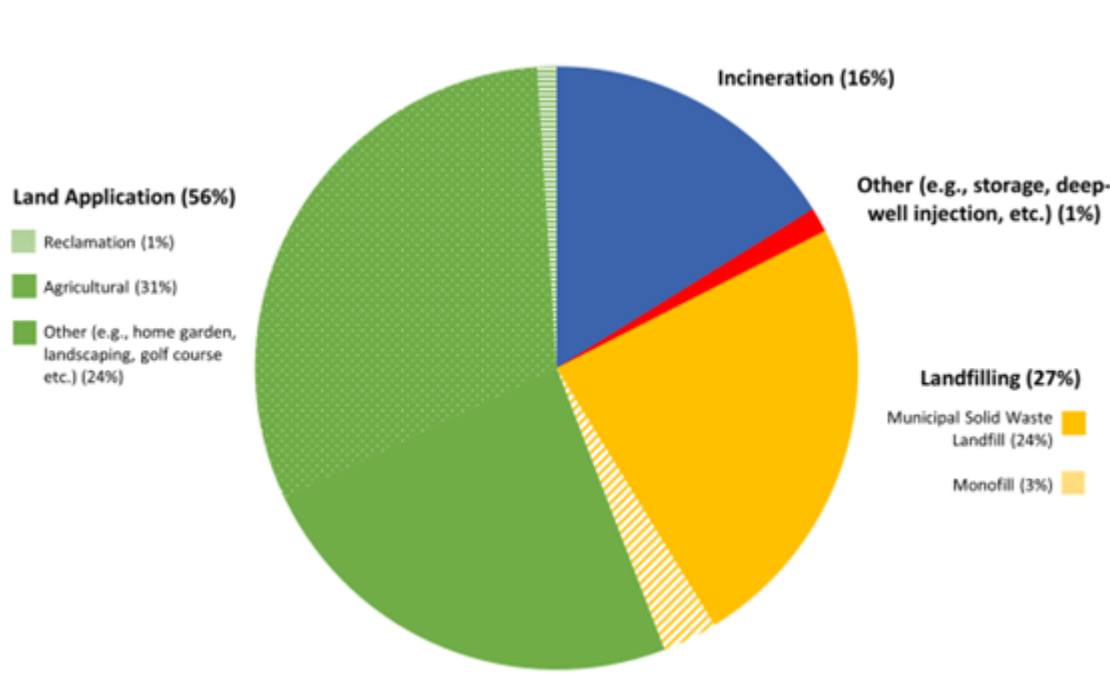


Figure 1.2. Biosolids Use & Disposal from 2022 Biosolids Annual Reports [11]

Historically, land application has been the sustainable option for biosolids disposal and accounted for a large portion of disposal in the US for 2022 [11]. However, the EPA requires biosolids to meet pollution limits before land application [11]. Depending on the economic climate of the area, this additional treatment of biosolids makes land application no longer financially favorable. Landfilling is also a popular disposal method; however, limited space and high cost makes it increasingly unfavorable for biosolid disposal [9]. As a result, there is a growing need for sustainable alternatives for disposal and use of biosolids. The high carbon contents and availability of biosolids make it a promising option for carbon-based adsorbents. In addition to the source of carbon precursor, the preparation methods need to be considered to determine the materials overall cost and sustainability.

1.3.1 Hydrothermal Carbonization

Hydrothermal carbonization has many advantages over the conventional thermochemical methods including higher biomass conversion efficiency, use of non-conventional materials, increase in adsorption capacity of biochar, better porosity and functional groups and the removal or immobility of contaminants [15]. The parameters of commonly used thermochemical processes are outlined in Table 1.2.

Table 1.2: Thermochemical process characteristics (a: [27], b: [28], c: [30])

Process	Process Conditions		Product Yield (%)		
	Temperature range (°C)	Residence time	Char	Liquid	Gas
Combustion	850-950 ^b	0.5-2s ^b	15-20 ^c	-	80-90 ^c
Gasification	800-1000 ^a	10-20s ^a	10 ^a	5 ^a	85 ^a
Fast pyrolysis	500 ^a	1s ^a	12 ^a	75 ^a	13a
Slow Pyrolysis	400 ^a	hrs-weeks ^a	35 ^a	30 ^a	35a
HTC	150-250 ^a	1-12 hrs ^a	50-80 ^a	5-20 ^a	2-5 ^a

In addition to its favorable operating conditions, one of the unique qualities of HTC from other thermochemical processes is its ability to treat biomass with a high moisture content [16]. The drying process of biosolids is energy intensive, giving hydrothermal carbonization an economic advantage over other methods [16]. HTC is an exothermal process that produces a concentrated carbonaceous material by dehydration and

decarboxylation [17]. The primary product is an energy-dense, porous solid known as Hydrochar [17].

This report outlines the experimental results for the adsorption capacity of sewage sludge based hydrochar with aqueous lead. In addition, these results are compared with previous work on the adsorption capacity of sewage sludge hydrochar with aqueous copper [18]. The hydrochar used for the lead experiments in this report as well as the previous work with copper referenced herein, is provided by SoMax Circular Solutions, a small company located in Pennsylvania that focuses on “converting organic waste to green solutions” [19].

1.4 Previous work

The Timko research group has previously worked with SoMax Hydrochar and Hydrochar in general. One such work by Hunter Wieckowski specifically looked at the adsorption capacity of unmodified and KOH modified SoMax sewage sludge hydrochar for copper [18]. Wieckowski also sought to characterize the SoMax hydrochar to identify the mechanisms by which copper adsorbs to the hydrochar. Wieckowski found KOH activation increased the max adsorption capacity of the hydrochar by more than double. It was concluded from the characterization methods that the KOH activation increased oxygenated functional groups and decreased the ash content [18].

2. Methods

The following section describes the procedures that were used to measure the adsorption capacity of the SoMax sewage sludge hydrochar. These lead adsorption methods were adapted from Hunter Wieckowski's work on copper adsorption [18]. The adsorption capacity of sewage sludge hydrochar was examined for initial concentrations of lead in the range of 50-800 ppm. All volumetric measurements greater than 2 mL were measured using a graduated cylinder of appropriate size. All measurements less than 2 mL were measured out using a 100-1000 μ L micropipette.

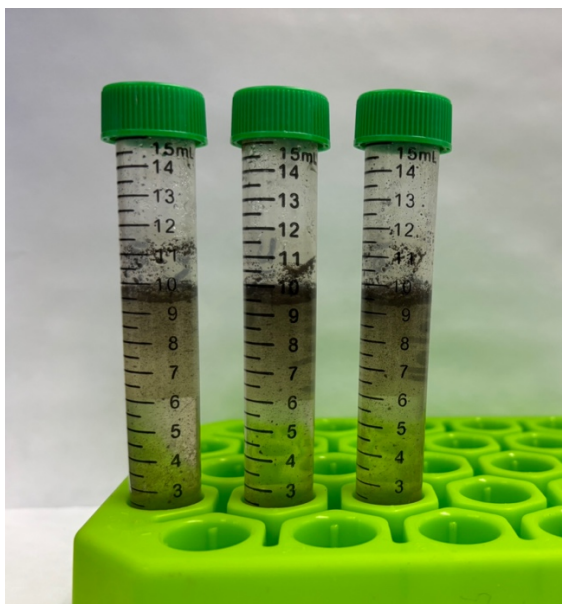
2.1 Sample Adsorption

To start, a 0.05 M stock solution of lead (II) nitrate was created by measuring out $8.2867\text{g} \pm 0.0001\text{g}$ of solid lead (II) nitrate and dissolving it in 500 mL of filtered deionized (DI) water. This solution was then diluted to create three other stock solutions of 0.005 M, 0.002 M and 0.0005 M to accommodate the small sample concentrations of 50-800 ppm (0.00024-0.00386 M). Liang et.al found hydrochar to be most effective in a solution with a pH of 5 [33]. A 495 mL acetic acid buffer solution was created with 11.3 g of sodium acetate dissolved in 490 mL of pure DI water and 5 mL of 17.4 M acetic acid. Using a calibrated pH meter, the final pH of the buffer solution was measured at a pH of 4.85. The pH of the buffer solution was re-measured frequently to ensure the pH had not changed.

Once the stock solutions were made, the samples were prepared with various starting concentrations of lead. For each concentration, four samples were prepared: three replicates and one control (no hydrochar). Each sample was prepared in a 15 mL

plastic centrifuge tube. 0.200 g of hydrochar was measured out for each triplicate sample and 45 mL of lead-buffer solution of a desired initial concentration was prepared. Lastly, 10 mL of the pre-prepared lead-buffer solution of a specified concentration was added to each of the four samples. To facilitate adsorption, each sample was placed in a mechanical shaker for a minimum of 24 hours. Figure 2.1 shows the samples with hydrochar before and after shaking.

(a)



(b)

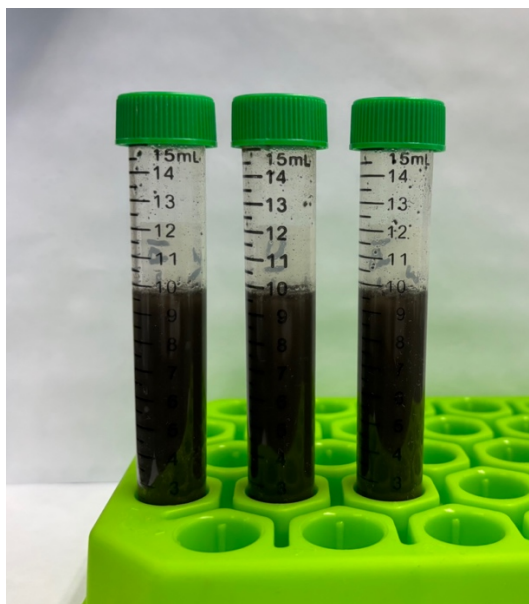


Figure 2.1. (a) samples with hydrochar before shaking and (b) samples with hydrochar after shaking

2.2 Sample Filtration and Dilution

After shaking for 24 hours, the samples were removed from the shaker for filtering. Filtration immediately after shaking is crucial to ensure that the adsorption time is constant for all samples. The samples must undergo an extensive filtration process to ensure there are no suspended solids, as this would damage the measurement device. The filtration process includes double vacuum filtration followed by syringe filtration. The vacuum

filtration process filters out the larger components of the hydrochar and the syringe filter removes any hydrochar particles leftover after vacuum filtration. The vacuum filtration process consists of a 100 or 150 mL Büchner flask fitted with a Büchner funnel. The Büchner flask was connected to a vacuum pump as seen in Figure 2.2.

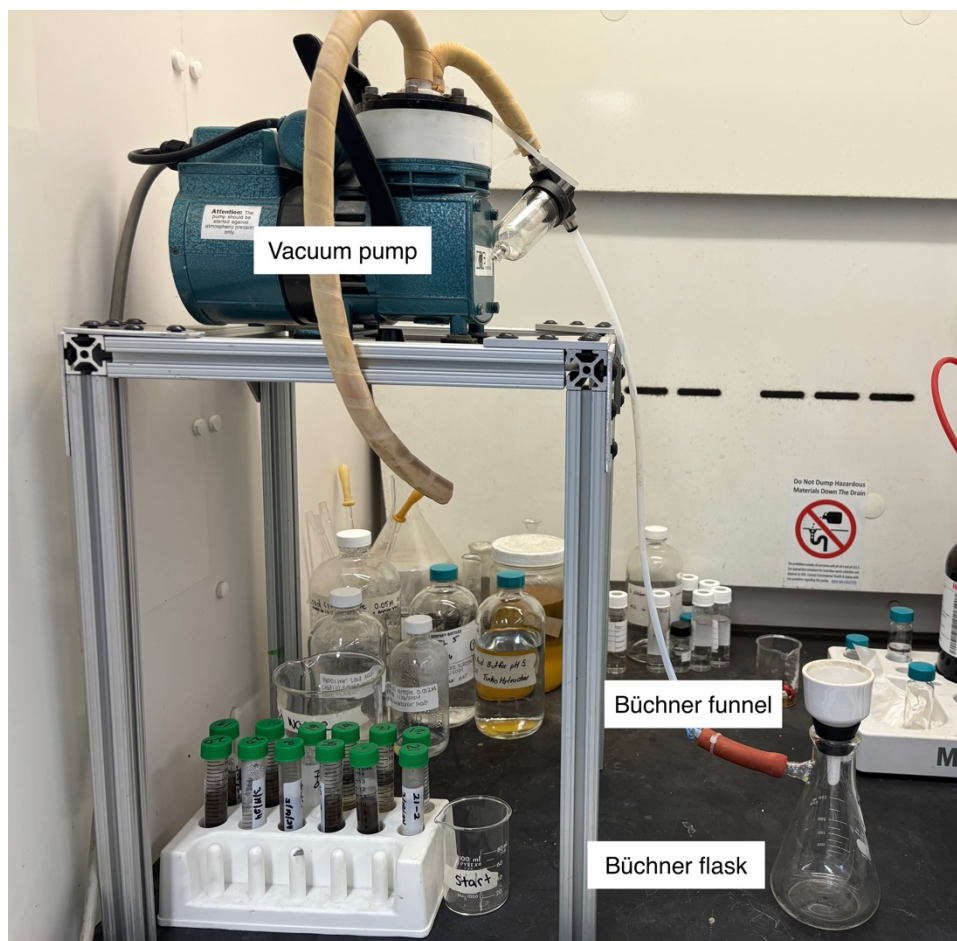


Figure 2.2. Vacuum filtration apparatus.

Filter paper (42.5 mm diameter) was dampened with 1-2 drops of water and placed in the funnel. The filter paper was properly sealed to the funnel to prevent leaks. The sample was carefully poured into the funnel and the vacuum pump was turned on. The

vacuum pump ran for approximately one minute or until the hydrochar on the filter paper appeared dry. The Büchner flask was detached from the pump and the filtrate was transferred to a clean beaker. The filter paper was replaced, and the glassware was thoroughly rinsed and dried between each run. After each sample was vacuum filtered twice, they were filtered once more using a 12 mL syringe and a 25 mm 0.02-micron syringe filter as seen in figure 2.3.



Figure 2.3. Syringe filtration of samples.

After filtration, the samples were diluted down to a concentration of 20-300 ppb due to limitations of the measurement device. Samples 1, 2 and 3 were diluted in a single dilution. Using the single dilution method resulted in significant waste and decreased accuracy. The serial dilution was used for the remainder of the samples. Each sample was serially diluted three to four times, each time by a factor of 10, depending on the starting concentration. The volume of the intermediate dilutions was 5.0 mL. The final

dilution volume was 9.5 mL and was placed into a clean centrifuge tube for data collection. The serial dilution process is shown in Figure 2.4.

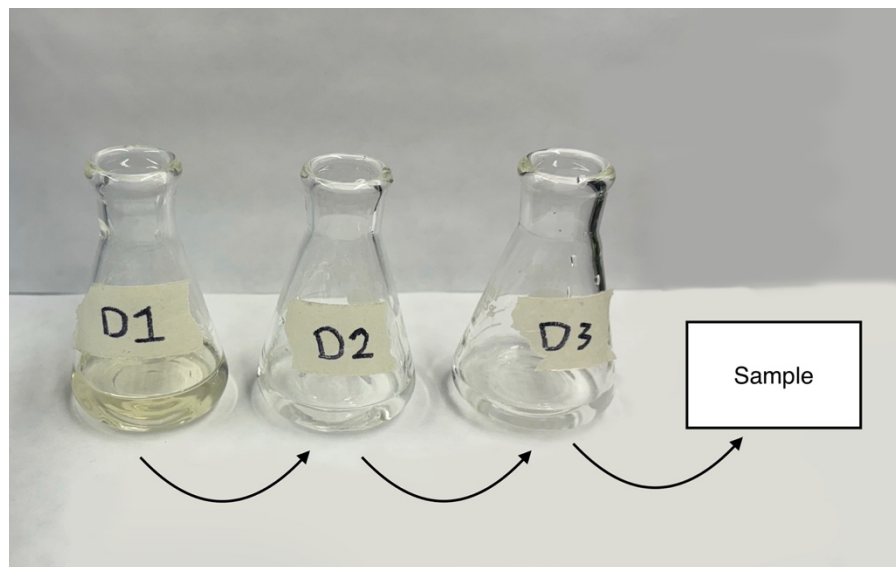


Figure 2.4. Diagram depicting the three serial dilutions performed for the experiments.

2.3 Measurement and Data Analysis

The concentration of lead in the samples was measured using the Perkin-Elmer Inductively Coupled Plasma mass spectrometer (ICP-ms) NexION 350x. The instrument requires strict sample regulation, including no dissolved solids, inorganic ion concentrations of 300 ppb or less and low pH. To ensure the samples had a low pH, 0.5 mL of Nitric acid was added to each sample before they were run through the ICP-ms. Prior to data collection, the machine was optimized using a set-up solution provided by the manufacturer. After the instrument was optimized, a series of standard solutions were measured to create a calibration curve. In addition to running a blank of DI water and a multi-ion NIST standard were run. The ICP-ms ran each sample in triplicates and averaged the values for the reported lead concentration in units of ppb. The concentration

in ppm was compared to the initial concentration to find the equilibrium concentration and adsorption capacity.

3. Results and Discussion

The difference of adsorption isotherm between SoMax sewage sludge hydrochar for lead and copper adsorbate can be found in Figure 3.1. The data for copper adsorption was collected by Hunter Wieckowski and will be used only for comparison purposes [18]. The calculated isotherms show lead exhibiting a higher adsorption capacity at an equilibrium concentration less than or equal to 0.1 mg/g. At an equilibrium concentration greater than 0.1 mg/g, the adsorption capacity for copper was significantly higher than lead, which aligns with the predictions from previous work [33].

Figure 3.1 A graph of adsorption capacity, Q_e , as a function of the equilibrium concentration, C_e . The data for both copper and lead are displayed with the calculated Langmuir and Freundlich adsorption models.

3.1 Lead Isotherm

The total data collected throughout the experiment summed to 16 points; each point representing the average of three replicates produced at the same conditions. The full isotherm can be seen in Figure 3.2. Three of these points were nullified due to errors in sampling and the dilution process. An over dilution caused the measured lead concentration to be significantly lower, where it was no longer within the ICP-ms calibration limits. The full isotherm including the removed data points (highlighted in red) is shown in Figure 3.3. The isotherms were recalculated after removing the qualitatively insignificant data and the final isotherm is shown in Figure 3.4.

Figure 3.3 A graph of the Adsorption capacity SoMax sewage sludge hydrochar, Q_e , as a function of the equilibrium concentration, C_e .

Figure 3.4. A graph of the Adsorption capacity SoMax sewage sludge hydrochar, Q_e , as a function of the equilibrium concentration, C_e . The graph only contains significant data.

3.2 Langmuir Adsorption

The Langmuir Isotherm is model of adsorption that assumes the surface of the adsorbent is homogeneous and can only adsorb a single molecular level [34]. The Langmuir model equation is often followed during chemical adsorption especially with ionic and covalent bonding between adsorbent and adsorbate. Equation 3.1 is used to model the Langmuir isotherm of lead adsorption.

$$Q_e = \frac{q_m K_L C_e}{1 + K_L C_e}$$

Equation 3.1: Langmuir Isotherm Equation [34]

The two unknown variables in Equation 3.1 were q_m and K_L . These variables were calculated from a line of best fit of the linearization of the adsorption data which can be seen in Figure 3.5. Equation 3.2 describes the linearization of the Langmuir equation.

Figure 3.5. The linearization of the lead adsorption data and line of best fit to find the Langmuir fit.

The graph in Figure 3.5 includes the equation of the line of best fit and the coefficient of determination (R^2). The line of best fit conforms to Equation 3.2.

$$\frac{C_e}{Q_e} = \frac{1}{q_m K_L} + \frac{1}{K_L} C_e$$

Equation 3.2: Linearization of the Langmuir Isotherm [34]

The maximum adsorption capacity is an effective factor to use when comparing different Langmuir isotherms [35]. Figure 3.6 is a graphical representation of the comparison of the max adsorption capacity for both copper and lead. The max adsorption

capacity of the Langmuir model isotherm for lead is 9.13 ± 0.621 mg of Pb/g which is one-fourth of the max adsorption capacity of copper which is 46.3 ± 7.18 mg of Cu/g.

Figure 3.6. A graphical comparison of the maximum adsorption, q_m , of both lead and copper for the adsorption as modeled by the Langmuir isotherm.

3.3 Freundlich Adsorption

The Freundlich isotherm is a model for adsorption that assumes the surface of the adsorbent is heterogeneous and is capable of multilayer adsorption, allowing for multiple adsorbates to bond to the same adsorption sites [36]. Equation 4.3 is used to model the Freundlich isotherm.

$$Q_e = K_F C_e^{1/n}$$

Equation 3.3: Freundlich Isotherm Equation [35]

To model the Freundlich isotherm for the data, $1/n$ and K_F need to be calculated. These variables were found through a line of best fit of the linearization of the adsorption data which can be seen in Figure 3.7. Equation 3.4 describes the linearization of the Langmuir equation.

Figure 3.6. The linearization of the lead adsorption data and line of best fit to find the Freundlich variables.

The graph in Figure 3.6 includes the equation of the line of best fit and the coefficient of determination. The line of best fit conforms to Equation 3.4.

$$\log Q_e = \frac{1}{n} \log C_e + \log K_F$$

Equation 3.4: Linearization of the Freundlich Isotherm [35]

K_F is an effective variable when comparing two Freundlich Isotherms [37]. The Freundlich adsorption coefficient is 21.8 ± 3.38 for the copper isotherm and 6.70 ± 2.22 for the lead isotherm. Figure 3.8 provides a graphical representation of the comparison of the Freundlich adsorption coefficients for both copper and lead.

Figure 3.8 A graphical comparison of the Freundlich adsorption coefficient, K_F , of both lead and copper for the adsorption as modeled by the Freundlich isotherm.

3.4 Comparisons to Additional Hydrochar

To better understand the adsorption behavior of the sewage sludge hydrochar for lead, the results from this set of experiments were compared to the results of lead adsorption for other hydrochar materials. The maximum adsorption capacities for the SoMax hydrochar compared to other types of hydrochar are shown in Figure 3.9.

Figure 3.9. The max adsorption capacity of SoMAX sewage sludge hydrochar (orange) compared to the values from other hydrochars (green).

Based on the results presented in this report, the sewage sludge hydrochar has a moderately high adsorption capacity when compared to other unmodified hydrochars. According to literature, KOH modification increases the adsorption capacity of modified hydrochar up to 3x higher than unmodified hydrochar [38]. Therefore, it is unsurprising that the KOH modified seaweed hydrochar had the highest adsorption capacity of 12.33 mg lead per gram hydrochar. Sewage sludge hydrochar exhibited higher adsorption capacity than peanut hull derived hydrochar, wheat straw derived hydrochar, and saw dust derived hydrochar. However, both wheat straw derived hydrochar and saw dust derived hydrochar were produced at high temperatures.

4. Conclusion

The goal of this work was to experimentally find the lead adsorption isotherm for SoMax sewage sludge hydrochar and compare it to the isotherm for the adsorption of copper for the same SoMax Hydrochar. For the adsorption of lead the Freundlich isotherm was found to have a slightly better fit with a coefficient of determination of 0.65 while the Langmuir model had a coefficient of determination of 0.63. However, due to relatively poor fits for both models, further work is recommended in order to make a strong conclusion from the data. In addition, other research has found the adsorption of lead with hydrochar to better follow the Langmuir model of adsorption. As result the discussion focuses more on comparisons using the Langmuir model. The max adsorption capacity (Langmuir) of lead was found to be 9.13 ± 0.62 mg Pb/g hydrochar while the copper max adsorption capacity was found to be 46.4 ± 0.18 mg Cu/g hydrochar. This aligns with previous work that found copper to be more favorable than lead during adsorption (Achilles). In addition, when the max adsorption capacity for sewage sludge hydrochar was compared to other hydrochars the sewage sludge hydrochar showed promising adsorption capacities and only falling short of a modified hydrochar material and a manure based hydrochar. However, the adsorption capacity of the unmodified sewage sludge hydrochar and unmodified manure based hydrochar were within 2 to 3 mg/g of the KOH modified seaweed hydrochar value, suggesting that the unique composition of organic waste and possible presence of potassium contribute to a higher adsorption capacity without any modification.

Throughout this process the team learned progress with experimental research is never linear and sometimes it is necessary to take a step back and rethink the process.

An example is that the team was able to streamline the dilution process to reduce the waste produced in addition to splitting up sample preparation to make it more manageable. In terms of the timeline for the project, the team was unable to begin testing until the second half of production duration due to issues related to the access and operability of the ICP-ms. Finally, the team learned that there is no such thing as bad data and that there is always something to learn from data even if the results were not what was expected.

5. Recommendations

Due to the small data sets for each concentration (3 data points) it is recommended that the experiments are replicated with at least 6-10 replicates for each concentration to increase the statistical accuracy of the data. In addition to increasing the number of replicates, it is also recommended that further work expand the range of concentrations examined beyond 800 ppm (initial concentration) in order to get a better idea of how and when the isotherm plateaus. Furthermore, it is also recommended that further work continues to investigate the adsorption capacities of both lead and copper at equilibrium concentrations less than 0.2 mg/g to either validate or invalidate the higher adsorption capacity for lead than copper at low concentrations.

Additionally, it is recommended that further work on this topic investigate the effect of different modifications on sewage sludge hydrochar. Previous work has found that KOH modification and the presence of potassium has a significant increased the adsorption capacity of hydrochar [18][40] Additionally, due to the high likelihood that potassium is already present in the material due to the nature of organic waste, it is recommended that further work look into the composition of sewage sludge and how the presence of

potassium in the unmodified hydrochar compares to various modified hydrochars. Furthermore, it is recommended that further characterization of the SoMax hydrochar is investigated to better understand the adsorption behavior of the hydrochar. Lastly, it is suggested that a new method of measuring the adsorbed lead is investigated as the PerkinElmer NexION ICP-ms required significant amounts of dilution and filtration which affected the number samples that were measured and the accuracy of the data points that were collected.

References

1. *Lead poisoning*. World Health Organization. <https://www.who.int/news-room/fact-sheets/detail/lead-poisoning-and-health#:~:text=Lead%20exposure%20is%20estimated%20to.>
2. Charkiewicz, A. E.; Backstrand, J. R. Lead Toxicity and Pollution in Poland. *International Journal of Environmental Research and Public Health* **2020**, *17* (12), 4385. <https://doi.org/10.3390/ijerph17124385>.
3. Kumar, V.; Dwivedi, S. K.; Oh, S. A Critical Review on Lead Removal from Industrial Wastewater: Recent Advances and Future Outlook. *Journal of Water Process Engineering* **2022**, *45*, 102518. <https://doi.org/10.1016/j.jwpe.2021.102518>.
4. Kumar, A.; Kumar, A.; M. M.s., C.-P.; Chaturvedi, A. K.; Shabnam, A. A.; Subrahmanyam, G.; Mondal, R.; Gupta, D. K.; Malyan, S. K.; Kumar, S. S.; A. Khan, S.; Yadav, K. K. Lead Toxicity: Health Hazards, Influence on Food Chain, and Sustainable Remediation Approaches. *International Journal of Environmental Research and Public Health* **2020**, *17* (7), 2179. <https://doi.org/10.3390/ijerph17072179>.
5. United States Environmental Protection Agency. *Learn about Lead | US EPA*. US EPA. <https://www.epa.gov/lead/learn-about-lead>.
6. US EPA. *Basic Information about Lead in Drinking Water | US EPA*. United States Environmental Protection Agency. <https://www.epa.gov/ground-water-and-drinking-water/basic-information-about-lead-drinking-water>.
7. Qasem, N. A. A.; Mohammed, R. H.; Lawal, D. U. Removal of Heavy Metal Ions from Wastewater: A Comprehensive and Critical Review. *npj Clean Water* **2021**, *4* (1), 1–15. <https://doi.org/10.1038/s41545-021-00127-0>.
8. Naidu, R. Inorganic Contaminants and Radionuclides; Elsevier, 2023; pp. 1–10
9. Rorat, A.; Courtois, P.; Vandenbulcke, F.; Lemiere, S. Sanitary and Environmental Aspects of Sewage Sludge Management. *Industrial and Municipal Sludge* **2019**, 155–180. <https://doi.org/10.1016/B978-0-12-815907-1.00008-8>.
10. Penn State Extension. *What is sewage sludge and what can be done with it?* Penn State Extension. <https://extension.psu.edu/what-is-sewage-sludge-and-what-can-be-done-with-it>.
11. US EPA. *Basic Information about Biosolids*. US EPA. <https://www.epa.gov/biosolids/basic-information-about-biosolids>.
12. Fic, K.; Platek, A.; Piwek, J.; Frackowiak, E. Sustainable Materials for Electrochemical Capacitors. *Materials Today* **2018**, *21* (4), 437–454. <https://doi.org/10.1016/j.mattod.2018.03.005>.

13. Duan, C.; Ma, T.; Wang, J.; Zhou, Y. Removal of Heavy Metals from Aqueous Solution Using Carbon-Based Adsorbents: A Review. *Journal of Water Process Engineering* **2020**, *37*, 101339. <https://doi.org/10.1016/j.jwpe.2020.101339>.
14. Basu, P. *Biomass Gasification, Pyrolysis and Torrefaction*, Third.; Academic Press, 2018; pp. 155–187.
15. Hong Nam Nguyen; Duy Anh Khuong. New Trends in Pyrolysis Methods: Opportunities, Limitations, and Advantages. **2022**, 105–126. https://doi.org/10.1007/978-981-19-2488-0_7.
16. Pauline, A. L.; Joseph, K. Hydrothermal Carbonization of Organic Wastes to Carbonaceous Solid Fuel – a Review of Mechanisms and Process Parameters. *Fuel* **2020**, *279*, 118472. <https://doi.org/10.1016/j.fuel.2020.118472>.
17. Funke, A.; Ziegler, F. Hydrothermal Carbonization of Biomass: A Summary and Discussion of Chemical Mechanisms for Process Engineering. *Biofuels, Bioproducts and Biorefining* **2010**, *4* (2), 160–177. <https://doi.org/10.1002/bbb.198>.
18. Wieckowski, H. *Characterization of Sewage Sludge Hydrochar for Use as a Heavy Metal Adsorbent*. Digital WPI. <https://digital.wpi.edu/concern/etds/9k41zj358?locale=en> (accessed 2024-04-08).
19. *SoMax Circular Solutions*. SoMax Circular Solutions. <https://somaxhtc.com> (accessed 2024-04-18).
20. Das, S.; Kaniz Wahida Sultana; A.R. Ndhlala; Mondal, M.; Chandra, I. Heavy Metal Pollution in the Environment and Its Impact on Health: Exploring Green Technology for Remediation. *Environmental health insights* **2023**, *17*. <https://doi.org/10.1177/11786302231201259>.
21. Burakov, A. E.; Galunin, E. V.; Burakova, I. V.; Kucherova, A. E.; Agarwal, S.; Tkachev, A. G.; Gupta, V. K. Adsorption of Heavy Metals on Conventional and Nanostructured Materials for Wastewater Treatment Purposes: A Review. *Ecotoxicology and Environmental Safety* **2018**, *148*, 702–712. <https://doi.org/10.1016/j.ecoenv.2017.11.034>.
22. Raji, Z.; Karim, A.; Karam, A.; Seddik Khalloufi. Adsorption of Heavy Metals: Mechanisms, Kinetics, and Applications of Various Adsorbents in Wastewater Remediation—a Review. *Waste* **2023**, *1* (3), 775–805. <https://doi.org/10.3390/waste1030046>.
23. Wang, B.; Lan, J.; Bo, C.; Gong, B.; Ou, J. Adsorption of Heavy Metal onto Biomass-Derived Activated Carbon: Review. *RSC Advances* **2023**, *13* (7), 4275–4302. <https://doi.org/10.1039/d2ra07911a>.
24. Fei, Y.; Yun Hang Hu. Design, Synthesis, and Performance of Adsorbents for Heavy Metal Removal from Wastewater: A Review. **2022**, *10* (3), 1047–1085. <https://doi.org/10.1039/d1ta06612a>.

25. Yang, X.; Wan, Y.; Zheng, Y.; He, F.; Yu, Z.; Huang, J.; Wang, H.; Ok, Y. S.; Jiang, Y.; Gao, B. Surface Functional Groups of Carbon-Based Adsorbents and Their Roles in the Removal of Heavy Metals from Aqueous Solutions: A Critical Review. *Chemical Engineering Journal* **2019**, *366*, 608–621. <https://doi.org/10.1016/j.cej.2019.02.119>.
26. Torres Pérez, M. D.; Kraan, S.; Domínguez González, H. *Sustainable Seaweed Technologies :Cultivation, Biorefinery, and Applications*; Elsevier: Amsterdam, 2020.
27. Libra, J. A.; Ro, K. S.; Kammann, C.; Funke, A.; Berge, N. D.; Neubauer, Y.; Titirici, M.-M.; Fühner, C.; Bens, O.; Kern, J.; Emmerich, K.-H. Hydrothermal Carbonization of Biomass Residuals: A Comparative Review of the Chemistry, Processes and Applications of Wet and Dry Pyrolysis. *Biofuels* **2011**, *2* (1), 71–106. <https://doi.org/10.4155/bfs.10.81>.
28. Nussbaumer, T. Combustion and Co-Combustion of Biomass: Fundamentals, Technologies, and Primary Measures for Emission Reduction†. *Energy & Fuels* **2003**, *17* (6), 1510–1521. <https://doi.org/10.1021/ef030031q>.
29. Sistemi a biomasse: progettazione e valutazione economica. Impianti di generazione di calore e di elettricità.iris.uniroma1.it. <https://iris.uniroma1.it/handle/11573/414812> (accessed 2024-04-24).
30. González-Arias, J.; Sánchez, M. E.; Cara-Jiménez, J.; Baena-Moreno, F. M.; Zhang, Z. Hydrothermal Carbonization of Biomass and Waste: A Review. *Environmental Chemistry Letters* **2021**, *20* (1), 211–221. <https://doi.org/10.1007/s10311-021-01311-x>.
31. *Sustainable Nanotechnology for Environmental Remediation*; Koduru, J. R., Karri, R. R., Mubarak, N. M., Bandala, E. R., Eds.; Elsevier BV, 2022; pp. 347–382. <https://doi.org/10.1016/c2020-0-01522-7>.
32. Liang, Y., Xu, D., Feng, P., Hao, B., Guo, Y., & Wang, S. (2021). Municipal sewage sludge incineration and its air pollution control. In *Journal of Cleaner Production* (Vol. 295, p. 126456).
33. Gatsonis, A. *Investigation of Heavy Metal Adsorption to Hydrothermal Char*. Digital WPI. https://digital.wpi.edu/concern/student_works/zw12z8581?locale=en (accessed 2024-04-23).
34. Liu, L.; Luo, X.-B.; Ding, L.; Luo, S.-L. 4 - Application of Nanotechnology in the Removal of Heavy Metal From Water. ScienceDirect. <https://www.sciencedirect.com/science/article/pii/B9780128148372000044>.
35. Vieira, J. C.; Soares, L. C.; R.E.S. Froes-Silva. Comparing Chemometric and Langmuir Isotherm for Determination of Maximum Capacity Adsorption of Arsenic by a Biosorbent. *Microchemical journal* **2018**, *137*, 324–328. <https://doi.org/10.1016/j.microc.2017.11.005>.

36. Sparks, D. L.; Singh, B.; Siebecker, M. G. Chapter 5 - Sorption Phenomena on Soils. ScienceDirect.
<https://www.sciencedirect.com/science/article/abs/pii/B9780443140341000058>.
37. Proctor, A.; Toro-Vazquez, J. F. The Freundlich Isotherm in Studying Adsorption in Oil Processing. *Journal of the American Oil Chemists' Society* 1996, 73 (12), 1627–1633. <https://doi.org/10.1007/bf02517963>.
38. Chen, H.; Yang, X.; Liu, Y.; Lin, X.; Wang, J.; Zhang, Z.; Li, N.; Li, Y.; Zhang, Y. KOH Modification Effectively Enhances the Cd and Pb Adsorption Performance of N-Enriched Biochar Derived from Waste Chicken Feathers. *Waste Management* 2021, 130, 82–92. <https://doi.org/10.1016/j.wasman.2021.05.015>.
39. Xue, Y.; Gao, B.; Yao, Y.; Inyang, M.; Zhang, M.; Zimmerman, A. R.; Ro, K. S. Hydrogen Peroxide Modification Enhances the Ability of Biochar (Hydrochar) Produced from Hydrothermal Carbonization of Peanut Hull to Remove Aqueous Heavy Metals: Batch and Column Tests. *Chemical Engineering Journal* 2012, 200-202, 673–680. <https://doi.org/10.1016/j.cej.2012.06.116>.
40. Ghanim, B.; O'Dwyer, T. F.; Leahy, J. J.; Willquist, K.; Courtney, R.; Pembroke, J. T.; Murnane, J. G. Application of KOH Modified Seaweed Hydrochar as a Biosorbent of Vanadium from Aqueous Solution: Characterisations, Mechanisms and Regeneration Capacity. *Journal of Environmental Chemical Engineering* 2020, 8 (5), 104176. <https://doi.org/10.1016/j.jece.2020.104176>.
41. Nzediegwu, C.; Naeth, M. A.; Chang, S. X. Lead(II) Adsorption on Microwave-Pyrolyzed Biochars and Hydrochars Depends on Feedstock Type and Production Temperature. *Journal of Hazardous Materials* 2021, 412, 125255. <https://doi.org/10.1016/j.jhazmat.2021.125255>.